

Large scale CO emission in the Orion Nebula

Núria Marcelino^{1,2}, Olivier Berné³, and José Cernicharo¹

¹ Centro de Astrobiología (CSIC-INTA), Ctra de Ajalvir km 4, 28850 Madrid, Spain

² National Radio Astronomy Obs., 520 Edgemont Rd, Charlottesville, VA 22903, USA

³ Leiden Obs., Leiden University, PO Box 9513, NL-2300 RA Leiden, The Netherlands

Abstract

We present ^{12}CO and ^{13}CO $J = 2 - 1$ large scale maps of Orion A observed with the IRAM 30-m radiotelescope. The size of the maps is $1^\circ \times 0.8^\circ$ at its largest extent, and their angular and velocity resolutions ($11''$ and $\sim 0.4 \text{ km s}^{-1}$, respectively) are higher than those used in previous extended CO maps of Orion. Besides a very complex velocity structure, these maps show numerous filaments and gas condensations, cometary globules and cavities (or tunnels). All these are signatures of the feedback action of massive star formation on the preexisting molecular gas. Among them, the detection of periodic structures on the surface of an elongated molecular cloud, provide evidence of the development of hydrodynamical instabilities shaping the molecular cloud. The discovery of these “waves” shows the high angular and spectral resolution required to understand star formation processes.

1 Introduction

The Orion molecular complex is the prototypical star forming region, because of its proximity and vigorous star formation activity. Thus it has been the subject of many studies at different wavelengths, from radio and millimeter wavelengths to the infrared, optical and X-ray emission (see [1, 6] for a review). This giant molecular cloud is a star nursery. Young massive stars and their strong stellar winds shape the parental molecular cloud, producing the collapse of new gas condensations and therefore triggering the formation of new stars. Fingerprints of star formation processes can be found everywhere in the cloud: hot cores, HII regions, circumstellar disks, outflows, Herbig-Haro objects, photodissociation regions, etc. All them reveal the strong interaction between young protostars and its surroundings.

The most abundant molecular species in the universe is H_2 , followed by carbon monoxide (CO). However because the lack of dipole moment, H_2 can not be observed at the cold and dense conditions where this species exist. On the other hand, the rotational transitions of

the asymmetric molecule CO, observable at millimeter and submillimeter wavelengths, provide the best way to study the distribution and kinematics of molecular gas in the universe. Indeed while the more abundant and optically thick isotopomer ^{12}CO probes the kinematics and can be used to measure the temperature of the cloud, the less abundant and optically thin isotopologues such as ^{13}CO and C^{18}O probe the column density of the gas along the line of sight. Although large scale ^{12}CO and ^{13}CO maps have been performed in Orion [9, 2, 4, 12], they lack either angular or spectral resolution enough in order to resolve the cloud structure and investigate in detail the kinematics of the cloud. Our new ^{12}CO and ^{13}CO $J = 2 - 1$ large scale maps were observed with both high angular ($\sim 11''$) and velocity ($\sim 0.4 \text{ km s}^{-1}$) resolutions, allowing us to resolve multiple line components and spatial structures at scales of 0.02 pc at a distance of 414 pc [11].

2 Observations

Observations were performed at the IRAM 30 m telescope (Granada, Spain) in March, April and October 2008. We used the 3×3 HERA receiver array, each polarization tuned to ^{12}CO and ^{13}CO $J = 2 - 1$ (230.5 and 220.4 GHz respectively) with image rejections ~ 10 dB. At these frequencies the beamwidth of the antenna is $\sim 11''$, and the main beam efficiencies are 0.524 and 0.545 for ^{12}CO and ^{13}CO respectively. As a backend we used the versatile spectrometer VESPA with 320 kHz of spectral resolution, corresponding to a velocity resolution $\sim 0.4 \text{ km s}^{-1}$. We observed in *On-The-Fly* (OTF) mapping mode scanning in α , with $5''$ of data sampling, and with steps of $12''$ in δ . Intensity calibration was performed frequently (3–4 min) using two absorbers at different temperatures, resulting in system temperatures between 300–500 K. Atmospheric opacities were obtained from the measurement of the sky emissivity and the use of the ATM code [5, 14], and found to be between 0.1–0.2 which correspond to 1–3 mm of precipitable water vapor. The map is centered at the position of the infrared source IRc2 ($\alpha_{\text{J2000}} = 05^{\text{h}}35^{\text{m}}14.5^{\text{s}}$, $\delta_{\text{J2000}} = -05^{\circ}22'29.3''$). The reference position, located at an offset of $(-3600'', -1800'')$ respect to IRc2, was checked to be free of CO emission. The complete map is a composition of 63 submaps, being the total size of the map $1^{\circ} \times 0.8^{\circ}$. The total number of positions observed in the map are 99415, with an on-source integration time of 6 seconds each (~ 1 second at the edges of the map).

3 Gas distribution and kinematics

Figure 1 shows the ^{12}CO and ^{13}CO $J = 2 - 1$ emission for all velocities and at three mean-velocity ranges, which represent the blue shifted gas moving toward the observer, the central mean velocity gas, and red shifted gas respect to the velocity of the cloud. In general the distribution of the gas is clumpy and filamentary, and reveals a very complex velocity structure, which may be the consequence of the star formation activity taking place. The total integrated emission maps (upper panels) show that the bulk of the gas is distributed along the N-S molecular filament, known as the integral-shaped filament (ISF [2]). The Orion Molecular Cloud 1 (OMC-1), located behind the Orion Nebula, is the brightest region seen

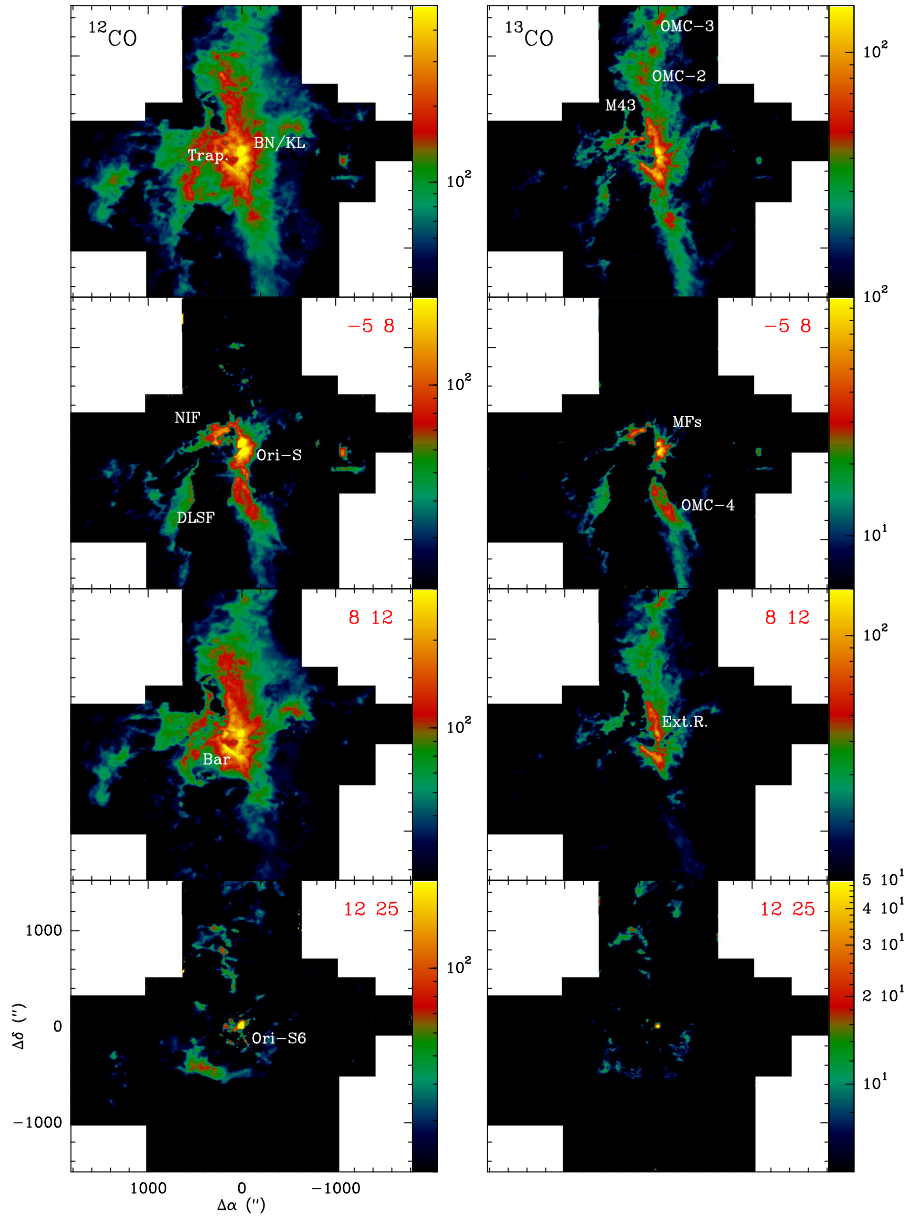


Figure 1: Observed ^{12}CO (left panels) and ^{13}CO (right panels) $J = 2 - 1$ emission distribution. Upper panels show the integrated emission for all velocities, while the panels below correspond to the observed emission at different velocity ranges, indicated in red in the upper right corner in each panel. Some of the most common features and regions within the Orion A cloud are indicated in the maps (see text.)

at the center of the filament and contains well-known features such as the BN-KL infrared nebula, the Extended Ridge (Ext.R.), the Orion-South region (Ori-S) and the Bar, which positions are indicated in the maps. In contrast to the bright emission of the Bar, the KL nebula and Ori-S, there is a small region of weak emission which corresponds to the location of the Trapezium stars. It is easy to see, in the ^{12}CO maps, the close relation of these bright features with the cone-like ionized structure of M42 observed in radio-continuum emission (see [24]). The ISF in the north contains the molecular clouds OMC-2/3, where many proto-stars and outflows have been detected (see [15]), and the HII region M43, seen as an empty cavity southwest to OMC-2. The gas distribution extends east and west of the main filament, but not equally. Whilst emission is truncated sharply southwest to the filament, coincident with a region where X-ray emission is observed [7], it spreads continuously toward east showing numerous clumps and filaments.

At the velocity range between -5 to 8 km s^{-1} (second row panels), we can see the gas moving toward the observer. The most prominent features, apart from the BN/KL object and Ori-S, are the bright filaments extending east and south from the center. The southern ISF contains an elongated clump of strong emission, OMC-4, which has also been found to be prominent in the IR [8]. Contrary to the north and central regions of the ISF, this clump is less turbulent and does not show signatures of on-going star formation (e.g. outflows). To the east there is another filament going northwest-southeast, which shows a very sharp and bright rim pointing towards the central region of the map. This long filament was first detected in CN $N = 1 - 0$ emission by [19]. These authors named this feature “Dark Lane South Filament” (DLSF) after the bright filament (Dark Lane) observed in the optical images of M42. Indeed, the DLSF should be related to the expansion of the HII region, as well as the other filament located north to DLSF also shown at these velocities. The latter is the counterpart of the north ionization front (NIF) of M42 and is connected to the molecular ridge at the north of the KL nebula. At the center of the map, going north and west from the BN/KL object and Ori-S, the so-called molecular fingers (MFs, see [18, 10]) are clearly seen in the ^{13}CO map. Further west, after an empty region, a spherical clump and an elongated structure (E-W) appear. These features, reported for the first time in this study, are only seen at these blue shifted velocities, suggesting that they are being pushed by a bubble of hot and ionised gas from massive stars. Indeed the elongated cloud is composed of several clumps which geometry and velocity suggest they are the result of a Kelvin-Helmholtz instability produced by the expansion of the nebula (see Section 4 and [3]). Whilst no significant emission is seen in ^{13}CO toward the north, we can see some clumps in ^{12}CO which are molecular outflows signatures, showing on-going star formation activity toward OMC-2/3.

At the mean cloud velocities ($8-12 \text{ km s}^{-1}$) the gas is mainly distributed at the central, northern and eastern parts of the map. We can see again the main features of the Orion Nebula, the OMC-2/3 clouds and M43. The red shifted emission however, looks completely different (lower panels). In the central region, we can see in the ^{12}CO map the bright BN/KL object together with many clumps and jets, revealing vigorous massive star formation activity taking place in this region. The Ori-S6 molecular outflow, clearly seen in the map as a highly collimated $2'$ long jet, has been subject of many studies at mm wavelengths [20, 25] (and references therein). Slightly to the north we can also see in the same panel other

outflows and star formation signatures, such as the two cometary globules which are located almost symmetrically respect to the center. These features should be related to the MFs, the optical filaments and the many Herbig-Haro (HH) objects detected in this region [10, 13]. At the northern end of the ISF we can see in ^{12}CO emission the red counterpart of the many molecular outflows arising in the star forming clouds OMC-2/3. The dense clumps associated with such activity are also seen in ^{13}CO . However, the most intriguing feature appears $10'$ south to NB/KL: a bubble-like structure which center looks to be located east of the KL nebula. This bubble of gas should be the result of the feedback interaction of star formation activity and the surrounding material which is pushed away from the observer either by the expansion of the HII region or by powerful star winds.

4 Kelvin-Helmholtz instabilities

Massive stars strongly disturb the parental cloud in which they are formed. Their energetic UV photons ionise and heat the preexisting molecular cloud, but they can also provoke compression and fragmentation of the cloud triggering the formation of a new generation of stars. However, further phenomena may arise from this mechanical interaction. The presence of large elongated structures in massive star forming regions, such as the “pillars of creation” and the Orion Molecular Fingers, have been suggested to be produced by hydrodynamical instabilities (*Spitzer* [23, 18]), however it has not been proved so far and other explanations are possible [16, 17]. The observation of wave-like structures on the surface of a molecular cloud is a key signature of such instabilities. The grown of the instability will eventually fragment the cloud in smaller globules or condensations which could undergo star formation. We have detected a series of five regular wavelets which are part of an elongated cloud, located southwest of the Orion molecular cloud.

Figure 2 shows a close-up view of the region in $^{12}\text{CO } J = 2-1$ at different velocities (red) overlaid with the Spitzer Infrared Array Camera (IRAC) $3.6 \mu\text{m}$ map (green). Both emissions show a coincident wave-like structure. The IR emission at $3.6 \mu\text{m}$ is attributed to the presence of polycyclic aromatic hydrocarbons (PAHs). A comparison between the spatial distribution of PAHs, H_2 0-0 S(1) pure rotational line intensity and ^{12}CO (2-1) emissions across the cloud shows a similar stratification than that expected in ultraviolet-driven photodissociation regions, with PAHs at the most external part of the cloud, followed by H_2 and ^{12}CO emissions [3]. The wavelets are subject to a strong velocity gradient ($7-9 \text{ km s}^{-1} \text{ pc}^{-1}$, see Fig. 2), which can not be explained by the simple expansion of the HII region ($\sim 3 \text{ km s}^{-1}$). Therefore it must result from the acceleration of the cloud produced by the mechanical interaction of high velocity plasma from massive stars with the molecular cloud, thus developing hydrodynamical instabilities. The simplest hydrodynamical instabilities which explain the observed structures are Rayleigh-Taylor and Kelvin-Helmholtz instabilities. The latter occur in an interface between fluids of different densities and velocities, as in the present case. [3] demonstrates that the development of KH instabilities is possible. However the effect of ultraviolet radiation from massive stars could prevent the instability to grow. Indeed, the extreme ultraviolet photons arising from Θ^1 Orionis C, the most luminous member of the Trapezium stars, could produce this effect. We conclude that the KH instability was formed before the birth of Θ^1

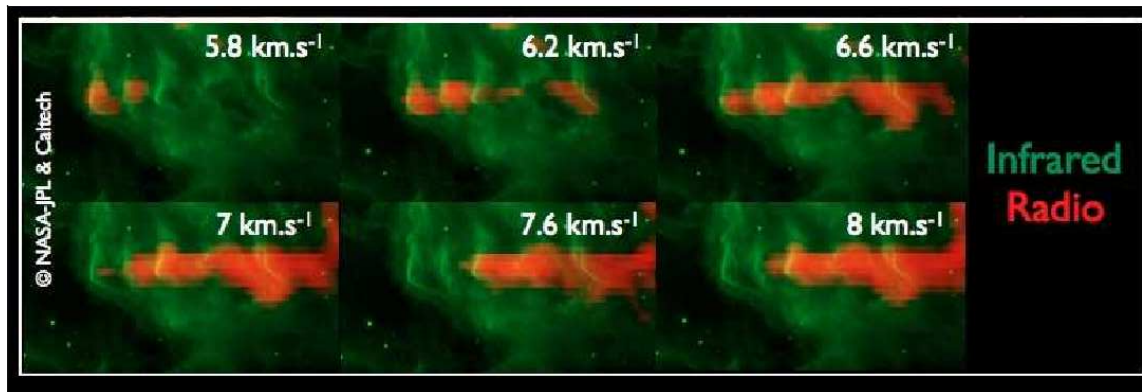


Figure 2: Overlay of the IRAM 30-m ^{12}CO emission at different velocities (red) and the Spitzer Infrared Array Camera (IRAC) $3.6\mu\text{m}$ map (green). The five wavelets are clearly seen in both emissions (see text).

Ori C, since at that time the photon flux would have been significantly lower than today. Therefore the expansion of dense HII gas produced by the population of older massive stars would have produced the KH instability. After the birth of Θ^1 Ori C, the introduction of intense radiation in the picture would have provoked a heterogeneous rocket acceleration [21, 22] of the clumps and the subsequent removal of the instability.

Acknowledgments

This work has been supported by Spanish Ministerio de Ciencia e Innovación through grants AYA2006-14876, ESP2007-65812-CO2-01, and by DGU of the Madrid community government under IV-PRICIT project S-0505/ESP-0237 (ASTROCAM).

References

- [1] Bally, J. 2008, in *Handbook of Star Forming Regions: Vol. I, The Northern Sky*, ed. Reipurth, B., ASP Monograph Publications, Vol.4, p.459
- [2] Bally, J., Langer, W.D., Stark, A.A., & Wilson, R.W. 1987, *ApJ*, 312, L45
- [3] Berné, O., Marcelino, N., & Cernicharo, J. 2010, *Nat*, 466, 947
- [4] Castets, A., Duvert, G., Dutrey, A., et al. 1990, *A&A*, 234, 469
- [5] Cernicharo, J. 1985, IRAM report No. 52 (Granada:IRAM)
- [6] Genzel, R., & Stutzki J. 1989, *ARA&A*, 27, 41
- [7] Güdel, M., Briggs, K.R., Montmerle, T., et al. 2008, *Sci*, 319, 309
- [8] Johnstone, D., & Bally, J. 1999, *ApJ*, 510, L49

- [9] Maddalena, R.J., Morris, M., Moscowitz, J., & Thaddeus, P. 1986, ApJ, 303, 375
- [10] Martín-Pintado, J., Rodríguez-Franco, A., & Bachiller, R. 1990, ApJ, 357, L49
- [11] Menten, K.M., Reid, M.J., Forbrich, J., & Brunthaler, A. 2007, A&A, 474, 515
- [12] Nagahama, T., Mizuno, A., Ogawa, H., & Fukui, Y. 1998, AJ, 116, 336
- [13] O'Dell, C.R., Hartigan, P., Lane, W.M., et al. 1997, AJ, 114, 730
- [14] Pardo, J.R., Cernicharo, J., & Serabyn, E. 2001, ITAP, 49, 1683
- [15] Peterson, D.E., & Megeath, S.T. 2008, in *Handbook of Star Forming Regions: Vol.I, The Northern Sky*, ed. Reipurth, B., ASP Monograph Publications, Vol.4, p.590
- [16] Pound, M.W. 1998, ApJ, 493, L113
- [17] Pound, M.W., Reipurth, B., & Bally, J. 2003, AJ, 125, 2108
- [18] Rodríguez-Franco, A., Martín-Pintado, J., Gomez-Gonzales, J., & Planesas, P. 1992, A&A, 264, 592
- [19] Rodríguez-Franco, A., Martín-Pintado, J., & Fuente, A. 1998, A&A, 329, 1097
- [20] Rodríguez-Franco, A., Martín-Pintado, J., & Wilson, T.L. 1999, A&A, 351, 1103
- [21] Ryutov, D.D., Kane, J.O., Pound, M.W., & Remington, B.A. 2003, Plasma Phys. Contr. Fusion, 45, 769
- [22] Ryutov, D.D., Kane, J.O., Mizuta, A., Pound, M.W., & Remington, B.A. 2007, Astrophys. Space Sci., 307, 173
- [23] Spitzer, L. 1978, *Physical Processes in the Interstellar Medium*, Wiley-Interscience
- [24] Yusef-Zadeh, F. 1990, ApJ, 361, L19
- [25] Zapata, L.A., Schmid-Burgk, J., Muders, D., et al. 2010, A&A, 510, A2